Swarm Expert Support Laboratories

Swarm L2 TEC Product Description

British Geological Survey (BGS)
National Space Institute – DTU Space (DTU)
Delft Institute of Earth Observation and Space Systems (DUT)
Helmholtz Centre Potsdam - German Research Centre for Geosciences (GFZ)
Eidgenössische Technische Hochschule Zürich (ETH)
Institut de Physique du Globe de Paris (IPGP)
The Swedish Institute of Space Physics (IRF)
Laboratoire d'électronique des technologies de l'information (Leti)
University of Calgary (UoC)
Aerospace Research And Test Establishment (VZLU)

with additional contributions from

NASA Goddard Space Flight Center (GSFC)
University of Colorado (CIRES)
Charles University Prague (CUP)

Doc. no: SW-TR-GFZ-GS-0007, Rev: 4, 2017-05-22

Contents

1 Document Change Log **3**

2 Applicable Documents **4**

3 Reference Documents **4**

4 Scope **5**

5 Introduction **5**
5.1 Algorithm 5
5.2 Scientific Relevance 5

6 Description of the data format **5**

7 Recomendation for using VTEC data **8**

8 Morphological comparison between STEC and electron density for representative examples **8**

9 Statistical Distribution of STEC and VTEC **12**

10 Conclusions **15**

1 Document Change Log

Issue	Issue Date	Pages Affected	Remarks	Author
1.0	27.08.2014	All	Initial Issue	J. Park
2.0	25.08.2016	7 8 12 13	two new variables in the table 1: Absolute-VTEC and Elevation-Angle New section 7 is inserted after section 6: old section 7 is now section 8 and so on Title and section text is modified in section 9 (old section 8) Figure 4 is replaced and new figure 5 is added	G. Kervalishvili
3.0	18.03.2017	5	TEC product document link is added	G. Kervalishvili
4.0	22.05.2017	12 12	H_{atmos} changed to H_{mapping} "... and H_{atmos} is assumed to be 400 km following RD1" text changed to "... and H_{mapping} is assumed to be 400 km RD1. This means that ..."	G. Kervalishvili

2 Applicable Documents

3 Reference Documents

RD1 Noja, M., C. Stolle, J. Park, and H. Lühr (2013), Long-term analysis of ionospheric polar patches based on CHAMP TEC data, Radio Sci., 48, 289-301, doi:10.1002/rds.20033.

RD2 Foelsche, U., and G. Kirchengast (2002), A simple "geometric"mapping function for the hydrostatic delay at radio frequencies and assessment of its performance, Geophys. Res. Lett., 29(10), doi:10.1029/2001GL013744.

RD3 Yizengaw, E., M. B. Moldwin, A. Komjathy, and A. J. Mannucci (2006), Unusual topside ionospheric density response to the November 2003 superstorm, J. Geophys. Res., 111, A02308, doi:10.1029/2005JA011433.

RD4 Swarm Level 2 Processing Facility Product specification for L2 Products and Auxiliary Products (SW-DS-DTU-GS-0001).

4 Scope

This document reports the results obtained from scientific quality validation of the Swarm Level-2 Total Electron Content product, TECATMS_2F, TECBTMS_2F and TECCTMS_2F.

Current or updated version of the TEC product description document is available on the EO web page: https://earth.esa.int/web/guest/document-library/browse-document-library/-/article/swarm-level-2-tec-product-description.

5 Introduction

5.1 Algorithm

The signals transmitted by the Global Navigation Satellite System (GNSS) satellites are delayed by ionospheric/plasmaspheric electrons before reaching the Swarm GNSS antenna. From the GNSS signal delay we can estimate slant total electron content (STEC), which is defined as 'integrated' electron density along the line of sight from Swarm to GNSS satellites. Relative STEC is given by the following equation:

$$STEC = \frac{f_1^2 f_2^2}{f_1^2 - f_2^2} \frac{L_1 - L_2}{K} \tag{1}$$

where f_1 and f_2 are carrier frequencies of GNSS signals, L_1 and L_2 are ambiguity-corrected carrier phase observations, and $K \approx 40.3$ m^{3}s^{-2}. After corrections for differential code biase of GNSS satellite transmitters and Swarm receivers, the relative STEC becomes absolute STEC. For complete description on the algorithm, readers are referred to RD1.

5.2 Scientific Relevance

L2-TEC data give integrated electron density along the line of sight from Swarm to GNSS satellites. The cadence of L2-TEC data is 1 Hz maximally, which is lower than that of the Swarm Level-1b (L1b) electron density data (EFIA_PL_1B, EFIB_PL_1B, and EFIC_PL_1B). However, as one Swarm satellite can communicate simultaneously with multiple GNSS satellites, there can be multiple STEC data points for a certain universal time (UT). Thanks to the wide spatial coverage at a given UT, the L2-TEC data can be a useful input to global ionospheric assimilations, which aim to specify 3-dimensional electron density structures.

6 Description of the data format

One data file of L2-TEC (TECATMS_2F, TECBTMS_2F or TECCTMS_2F) is produced per day and per Swarm satellite (Alpha, Bravo, or Charlie). An L2-TEC file is produced only when all the following input files are available: (1) GNSS RINEX observation files (GPSA_RO_1B, GPSB_RO_1B, or GPSC_RO_1B), (2) Swarm ephemerides (MODA_SC_1B, MODB_SC_1B, or MODC_SC_1B), (3) GNSS satellite

ephemerides (AUX_GPSEPH), and (4) differential code biase of GNSS satellite transmitters (AUX_DCB_2F).

The cadence of the L2-TEC data (TECATMS_2F, TECBTMS_2F and TECCTMS_2F) is variable: at the beginning of the mission it was 0.1 Hz, and it was changed into 1 Hz in July 2014. The following table presents the list of variables in the L2-TEC data product. The elevation angle of the GNSS satellites as seen from Swarm can be calculated using the two variables, 'GPS-Position' and 'LEO-Position'. For more complete description on the data content, readers are referred to RD1 and RD4.

Table 1: The list of variables in the L2-TEC data product.

Variable name	**Description**	**Unit**
Timestamp	Time stamps in Universal Time	cdf epoch
Latitude	Geographic latitude of the Swarm satellite	degree
Longitude	Geographic longitude of the Swarm satellite	degree
Radius	Distance of the Swarm satellite from the Earth's center	m
GPS-Position	X-, Y-, Z-coordinates of the GNSS satellite used for STEC calculation	m
LEO-Position	X-, Y-, Z-coordinates of the Swarm satellite used for STEC calculation	m
PRN	Pseudo-Random Number (PRN) identifier of the GNSS satellite used for STEC calculation	no unit
L1	GNSS L1 carrier phase observation	m
L2	GNSS L2 carrier phase observation	m
P1	GNSS P1 carrier phase observation	m
P2	GNSS P2 carrier phase observation	m
S1	GNSS signal-to-noise ratio or raw signal strength on L1	no unit
S2	GNSS signal-to-noise ratio or raw signal strength on L2	no unit
Absolute-STEC	Absolute slant TEC	TECU
Absolute-VTEC	Absolute vertical TEC	TECU
Elevation-Angle	Elevation angle	degree
Relative-STEC	Relative slant TEC	TECU
Relative-STEC-RMS	Root mean square error of relative slant TEC	TECU
DCB	GNSS receiver differential code bias	TECU
DCB-Error	Error in the GNSS receiver differential code bias	TECU

7 Recomendation for using VTEC data

It is recommended to use absolute VTEC data with corresponding elevation angles of the GPS rays of at least 50°. The elevation angle values are available in the standard L2-TEC files (Table 1). The recommendation is given since the uncertainty of the mapping function (Eq. 3) increases with decreasing elevation angle.

8 Morphological comparison between STEC and electron density for representative examples

Here we present some examples of L2-TEC data, and compare them with the electron density data obtained from the Langmuir Probe (LP) onboard Swarm. As STEC is electron density integrated along the line-of-sight between Swarm and the GNSS satellites, reasonable correlation between STEC and electron density is expected.

Figure 1 shows a typical example of Swarm L2-TEC data. The top panel presents STEC, middle panel, elevation angle of the GNSS satellite as seen from Swarm, and the bottom panel shows electron density measured by the Swarm/LP. Identifiers of the Swarm and GNSS satellites as well as magnetic local time (MLT) of the pass are given in the title. As Swarm was near local noon (MLT=12.23h), the electron density in the bottom panel exhibits clear signatures of the Equatorial Ionization Anomaly (EIA), which consists of double humps off the equator.

Figure 2 shows another example of L2-TEC and LP data comparison, and the figure format is the same as that of Figure 1. The corresponding MLT is near midnight, and we can see clear bubble structures in electron density between $-5° \sim +25°$ in geographic latitude (GLAT). In the top panel STEC exhibits similar profile to that of electron density although fine structures in the electron density profile are absent (note that STEC data rate is 0.1 Hz here).

Figure 3 shows an example at high latitudes, and the figure format is the same as that of Figure 1. The corresponding MLT is near noon, and we can see clear enhancement in electron density between $-80° \sim -70°$ in GLAT. In the top panel STEC exhibits similar profile to that of electron density although fine structures in the electron density profile are absent. Note that such density enhancement around noontime high-latitude regions is quite a common phenomenon as demonstrated by RD1.

From Figures 1-3 we can conclude that latitudinal profiles of STEC generally agree with those of electron density. This agreement support the reliability of the Swarm L2-TEC product.

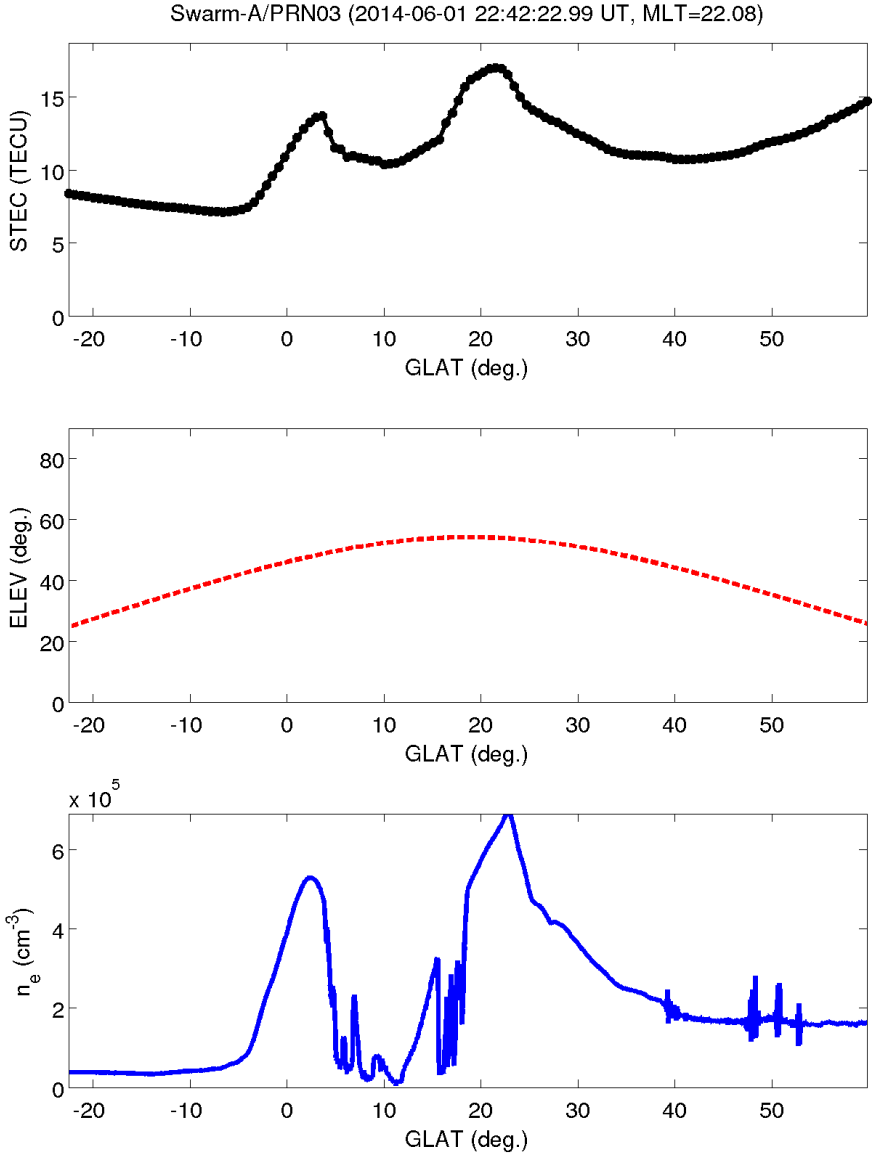

Figure 1: An example of Swarm L2-TEC data.

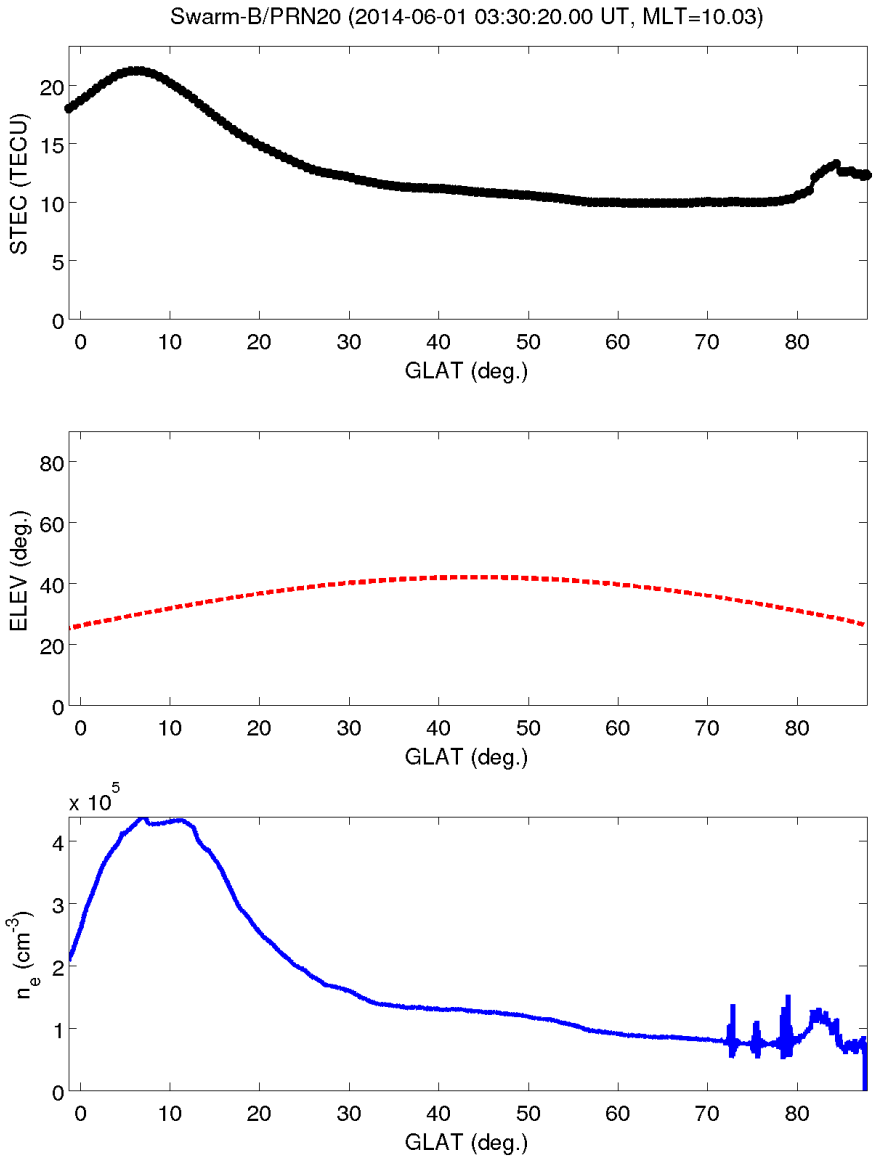

Figure 2: Another example of Swarm L2-TEC data.

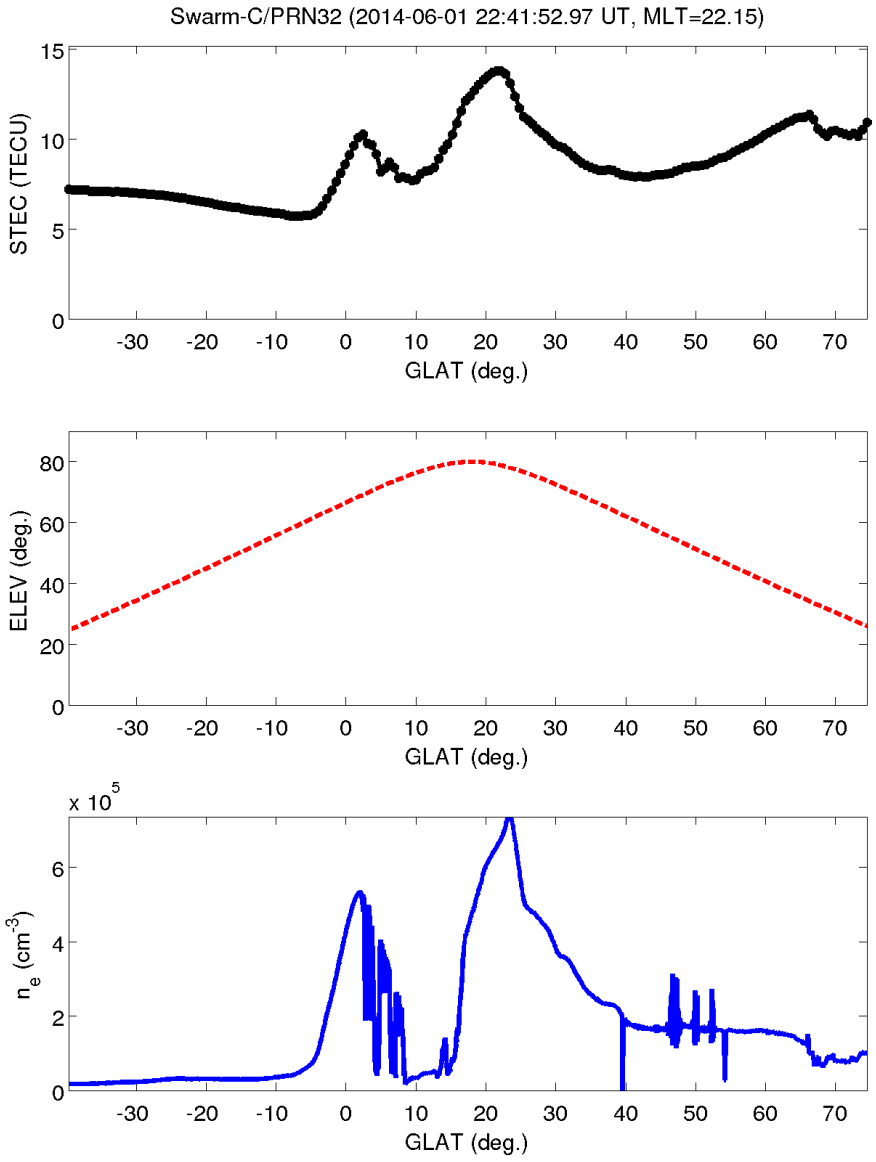

Figure 3: A high-latitude example of Swarm L2-TEC.

9 Statistical Distribution of STEC and VTEC

Figures 4 and 5 presents the statistical distribution (from July 2014 to April 2016) of absolute slant and absolute vertical TEC, STEC and VTEC with elevation angle values $> 70°$, respectively, as derived by the L2-TEC processor. The three panels correspond to Swarm-Alpha (A), -Bravo (B), and -Charlie (C), respectively. Absolute VTEC is defined from absolute STEC according to the following equations (RD2):

$$VTEC = STEC \cdot M(\epsilon), \tag{2}$$

$$M(\epsilon) = \frac{H_{\text{mapping}}}{R_{\text{Sw}} + H_{\text{mapping}}}[cos(sin^{-1}(r \times cos\epsilon)) - r \times sin\epsilon]^{-1}, \tag{3}$$

$$r = \frac{R_{\text{Sw}}}{R_{\text{Sw}} + H_{\text{mapping}}}, \tag{4}$$

where M is the mapping function (RD2), R_{Sw} is the radius of the Swarm (Swarm satellite altitude + radius of the Earth), ϵ is the elevation angle of the GNSS satellite as seen from Swarm, and H_{mapping} is assumed to be 400 km RD1. This means that the ionosphere is assumed to be a "thick shell" (height-independent plasma density with 400 km thickness) above the Swarm satellite.

For all Swarm satellites during the daytime and around the magnetic equator STEC (Fig. 4) and VTEC (Fig. 5) are higher than at any other MLT and MLAT. This is consistent with the fact that solar radiation is the prime source of ionospheric plasma, which is the main contributor to TEC. Around sunset (1800 LT) STEC and VTEC at low latitudes is enhanced again. This agrees with the well-known pre-reversal enhancement of ionospheric uplift, which can enhance TEC through reduced plasma recombination at high altitudes. Dayside and post-sunset peaks are better visible for VTEC, because STEC is averaging features. Maximum VTEC is about 25-28 TECU at low latitudes, which is in general agreement with VTEC from the CHAMP satellite (e.g., see Figure 6a of RD3). STEC and VTEC from Swarm A (top panel) and Swarm C (bottom panel) exhibits the same behavior in terms of the relative variation and absolute magnitude. This is as expected from the fact that Swarm A and Swarm C are at the same altitudes since mid-April 2014, with zonal separation of only about 1.5°GLON near the equator. STEC and VTEC from Swarm B (middle panel) exhibits nearly the same behavior as that of Swarm A and Swarm C, but the absolute magnitude of TEC is lower than for Swarm A and Swarm C. This is because Swarm B has been flying higher than the other two since mid-April 2014. As all three satellites are expected to fly above the peak altitude of ionospheric electron density (the F-layer peak), TEC should decrease significantly with observation altitude of satellites. In conclusion, the TEC properties shown in Figures 4 and 5 generally agree with expectations from the current knowledge on the ionosphere.

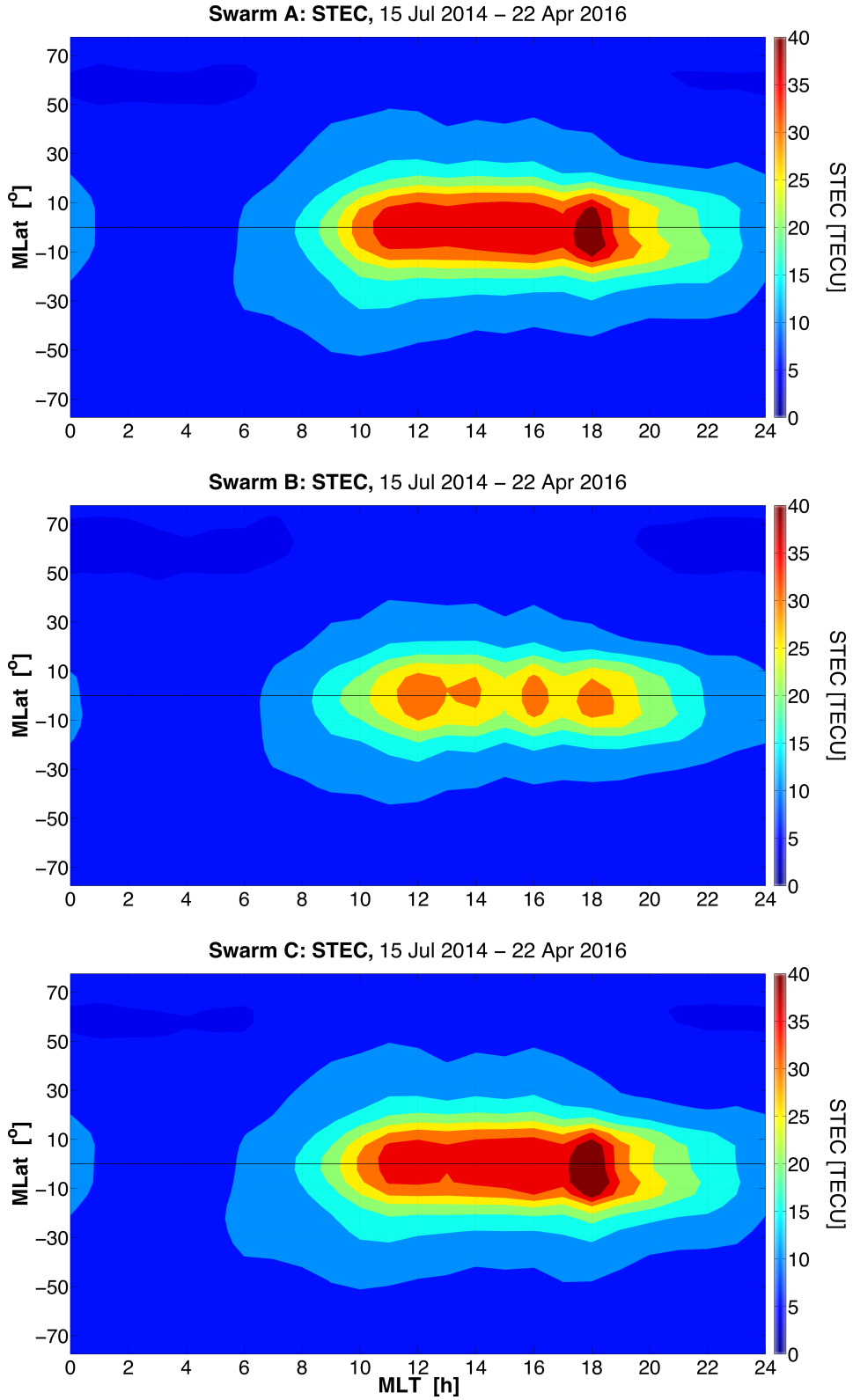

Figure 4: Statistical distribution of absolute STEC from the L2-TEC processor.

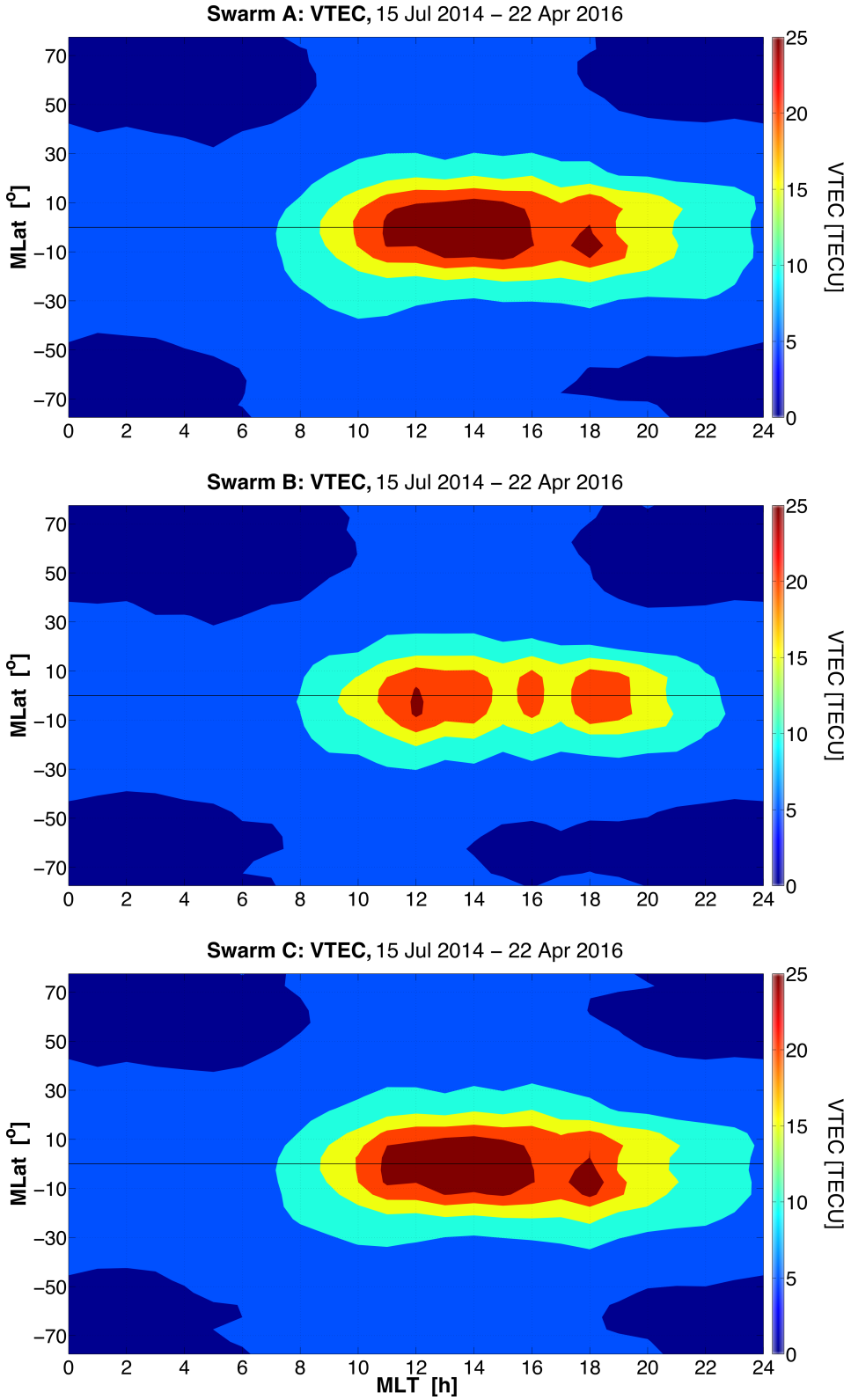

Figure 5: Statistical distribution of absolute VTEC derived from the L2-TEC processor.

10 Conclusions

The results obtained confirm the scientific validity of the L2-TEC data (TECATMS_2F, TECBTMS_2F or TECCTMS_2F).